Polyoxometalate-based gasochromic silica†

Bingbing Xu, Lin Xu,* Guanggang Gao, Zhikui Li, Yu Liu, Weihua Guo and Liping Jia

Received (in Montpellier, France) 31st January 2008, Accepted 3rd March 2008
First published as an Advance Article on the web 21st April 2008
DOI: 10.1039/b801764f

Materials capable of gasochromic behavior are still rare. In this paper, amorphous gasochromic hybrid silica material containing phosphomolybdic acid (PMo_{12}) is prepared by the sol–gel technique. The structure and properties of the material are investigated by cyclic voltammetry, thermal gravimetric analysis, FT-IR spectra, X-ray diffraction, UV-Vis spectra and X-ray photoelectron spectra. The structural integrity of phosphomolybdic acid has been preserved after incorporation into the porous silica framework. Furthermore, the PMo_{12}–SiO_2 hybrid material shows sensing activity for H_2S and SO_2 gases at room temperature based on the color change.

Introduction

Chromogenic materials are a type of smart material used for large area glazing, information displays, switch devices and optical storage. These technologies consist of electrically driven media involving electrochromism, suspended particle electrophonesis, polymer dispersed liquid crystals, electrically heated thermotropics and gasochromics.[1] Among the chromogenic materials, WO_3 can be gasochromic towards dilute H_2 with the noble metals Pt or Pd as catalysts.[2] Polyoxometalates (POMs) are a wide class of inorganic metal oxide clusters that have found many applications in the fields of catalysis, medicine, biology, molecular magnetism and materials science due to their rich topological, chemical and physical properties.[3] One of the most important electronic properties of the inorganic compound POMs is their ability to accept electrons to become colored mixed-valence species without any change in the original structure and the reduced species often display deep blue coloration, the heteropoly blues.[4] POMs can be considered as microcrystallites of hydrated $(WO_3)_n$ or $(MoO_3)_n$ which are well-organized around the heteroionic group. Upon reduction to heteropoly blues, they show properties similar to those of the respective infinite oxides.[5] These properties make them promising candidates for chromogenic materials. Therefore, taking account of the available electrons transfer between POMs and gas molecules, the development of POM-based gasochromic materials is of considerable feasibility and importance. In order to extend our previous work of exploring the electrochromic and photochromic properties based on POMs,[6] we are currently interested in the exploration of their gasochromism.

Key Laboratory of Polyoxometalates Science of Ministry of Education, College of Chemistry, Northeast Normal University, Changchun, 130024, P. R. China. E-mail: linxu@nenu.edu.cn; Fax: +86 431 8509 9668; Tel: +86 431 8509 9668

† Electronic supplementary information (ESI) available: The dependence of cathodic peak currents on scan rates and the square roots of scan rates for PMo_{12} aqueous-modified electrode and PMo_{12} sol-modified electrode (Fig. S1), XPS spectra of molybdenum and sulfur elements for the silica after exposure to SO_2 (Fig. S2), X-ray diffraction pattern of silica containing PMo_{12} (Fig. S3), and main relevant IR data observed for PMo_{12} and PMo_{12}–SiO_2 hybrid materials (Table S1). See DOI: 10.1039/b801764f

At present, monitoring air pollutants is an important aspect of industrial processing and environmental protection. In most cases, H_2S and SO_2 gases sensors mainly employ semiconductor metal oxides or solid electrolytes as the sensing material.[7] Despite enormous progress, many sensing systems still show disadvantages in terms of high cost and complicated device fabrication. In this paper, we report the preparation and characterization of a gasochromic silica sensing material containing POMs. The fabrication procedure of the gasochromic monolithic pieces is very simple. In addition, the advantage of the POMs-SiO_2 material is that it is capable of detecting some reducing gases at room temperature without any power consumption. To our knowledge, the gasochromic property of POMs is firstly investigated here, suggesting a new gas sensing material and potential application in chemical sensors.

Results and discussion

Phosphomolybdic acid $H_3PMo_{12}O_{40}{\cdot}24H_2O$ (PMo_{12}) having a Keggin structure consists of a central tetrahedral PO_4 surrounded by 12 molybdenum–oxygen octahedral MoO_6 units. The PMo_{12} material shows high solubility and reversible redox behavior.[3d,4b] The gasochromic material was prepared by incorporating the yellow PMo_{12} into a silica network by using a sol–gel method. During gelation, the large monolith cracks into small pieces.

Electrochemistry investigation

Comparative cyclic voltammetry (CV) curves of aqueous PMo_{12} and of sol-modified PMo_{12} are shown in Fig. 1(a) and (c), respectively. In the potential range from −0.12 to 0.6 V, three pairs of reversible redox waves were observed with formal potentials at E(I) = 0.317 V [E_{pc}(I) = 0.296 V, E_{pa}(I′) = 0.338 V], E(II) = 0.189 V [E_{pc}(II) = 0.177 V, E_{pa}(II′) = 0.201 V] and E(III) = −0.048 V [E_{pc}(III) = −0.072 V, E_{pa}(III′) = −0.024 V], where $2E = E_{pc} + E_{pa}$ (Fig. 1(a)). These waves I–I′, II–II′ and III–III′ correspond to reduction and oxidation of $PMo^{VI}{}_{12}O_{40}{}^{3-}$, $H_2PMo^{V}{}_2Mo^{VI}{}_{10}O_{40}{}^{3-}$, $H_4PMo^{V}{}_4Mo^{VI}{}_8O_{40}{}^{3-}$ and $H_6PMo^{V}{}_6Mo^{VI}{}_6O_{40}{}^{3-}$ through three two-electron redox processes, respectively.[8] The cyclic

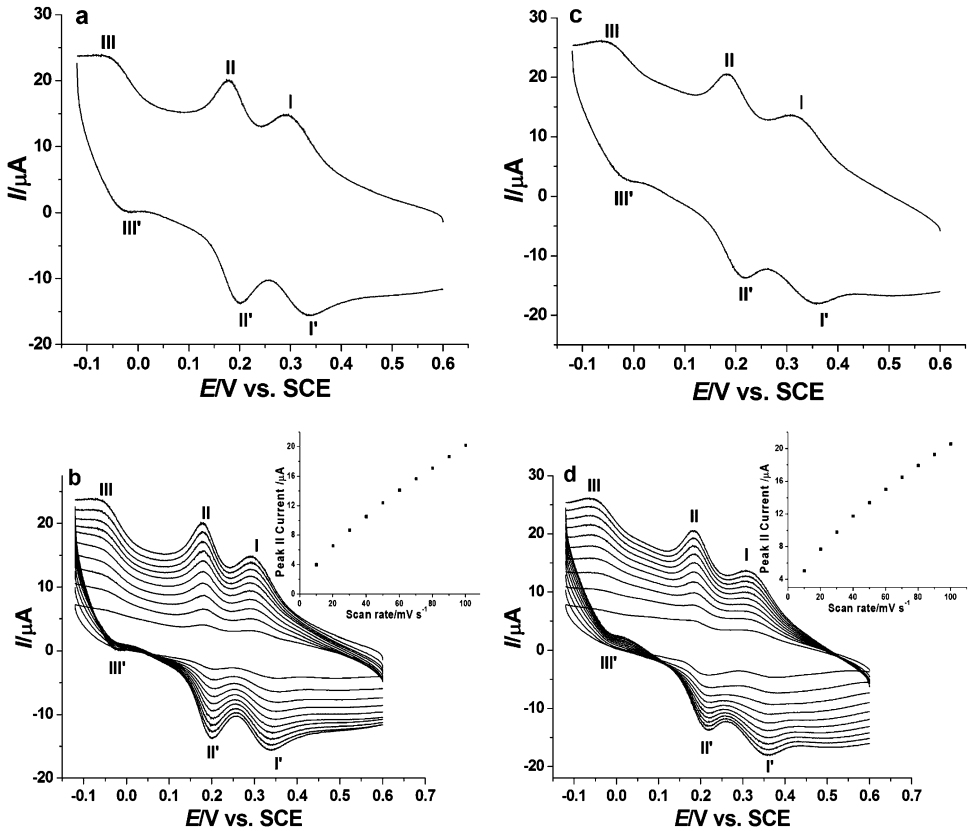

Fig. 1 Cyclic voltammetry of a glassy carbon electrode modified by PMo_{12} aqueous solution (a) at a scan rate of 100 mV s^{-1} and (b) at scan rates (inner to outer) of 10, 20, 30, 40, 50, 60, 70, 80, 90 and 100 mV s^{-1}. The inset shows the plot of cathodic peak currents *vs.* scan rates; Cyclic voltammetry of PMo_{12} sol-modified electrode (c) at a scan rate of 100 mV s^{-1} and (d) at scan rates (inner to outer) of 10, 20, 30, 40, 50, 60, 70, 80, 90 and 100 mV s^{-1}. The inset shows the plot of cathodic peak currents *vs.* scan rates.

voltammetry curve of the PMo_{12} sol-modified electrode shows three similar couples of redox waves as shown in Fig. 1(c). The formal potentials of the PMo_{12} sol-modified electrode are at E(I) = 0.339 V, [E_{pc}(I) = 0.320 V, E_{pa}(I′) = 0.358 V], E(II) = 0.202 V [E_{pc}(II) = 0.185 V, E_{pa}(II′) = 0.218 V] and E(III) = −0.037 V [E_{pc}(III) = −0.059 V, E_{pa}(III′) = −0.015 V], respectively. Fig. 1(b) and (d) show the CV curves of the PMo_{12}-modified electrodes at different scan rates in 0.5 M H_2SO_4 aqueous solution, and the insets display plots of cathodic peak currents *vs.* scan rates. As the scan rates were varied from 10 to 50 mV s^{-1}, the cathodic peak currents were proportional to the scan rates, indicating that the redox processes are surface-controlled. However, at scan rates higher than 50 mV s^{-1}, the cathodic peak currents were proportional to the square root of scan rates, suggesting that redox processes were diffusion-confined. The overall redox processes of PMo_{12}-modified electrode in acid solution are summarized as shown in eqns (1)–(3).

$$PMo^{VI}{}_{12}O_{40}{}^{3-} + 2e^- + 2H^+ = H_2PMo^{V}{}_2Mo^{VI}{}_{10}O_{40}{}^{3-} \quad (1)$$

$$H_2PMo^{V}{}_2Mo^{VI}{}_{10}O_{40}{}^{3-} + 2e^- + 2H^+ = H_4PMo^{V}{}_4Mo^{VI}{}_8O_{40}{}^{3-} \quad (2)$$

$$H_4PMo^{V}{}_4Mo^{VI}{}_8O_{40}{}^{3-} + 2e^- + 2H^+ = H_6PMo^{V}{}_6Mo^{VI}{}_6O_{40}{}^{3-} \quad (3)$$

These results indicate that the electrochemical property of PMo_{12} is maintained after incorporation into the silica network. Therefore, we infer that structural integrity of phosphomolybdic acid has been preserved after incorporation into the porous silica framework. The redox potentials of phosphomolybdic acid as well as pertinent sulfur species are given in Table 1. It is noted that phosphomolybdic acid has a sufficiently positive potential to be capable of oxidizing hydrosulfide cleanly in water.[9]

Thermal gravimetric analysis

It should be noted that high amount of water molecules in the monolithic pieces promote transport of hydrogen along the

Table 1 Potentials of phosphomolybdic acid and selected sulfur species

Species	E/V
$PMo_{12}O_{40}{}^{3-}$	0.320[a]
Hydrogen sulfide (S/H_2S)	0.142[b]
Hydrosulfide (S/S^{2-})	−0.478[b]
Sulfur ($S_2O_3{}^{2-}/S_8$)	−0.74[b]
Sulfite ($SO_4{}^{2-}/SO_3{}^{2-}$)	−0.93[b]
Thiosulfate ($SO_3{}^{2-}/S_2O_3{}^{2-}$)	−0.571[b]

[a] Reduction potential taken from cyclic voltammetry. [b] Standard reduction potentials *vs.* SHE; all values for the sulfur species taken from ref. 9.

PMo_{12} pore surface.[10] In addition, we can change the amount of water by adjusting the preparation conditions. The thermal gravimetric analysis (TGA) curves of phosphomolybdic acid and the hybrid silica material are shown in Fig. 2. The TGA profile for phosphomolybdic acid showed three distinct weight loss patterns. The first two weight losses from 50 to 120 °C corresponds to loss of non-coordinated and crystal water. The third loss centered at about 350 °C is the loss of all protons of phosphomolybdic acid and the beginning of decomposition of the Keggin structure. The TGA profile of silica material exhibits two weight loss patterns: an initial gradual weight loss from 30 to 150 °C by 18% is due to loss of surface water and the second weight loss from 300 to 500 °C of 5% is attributed to the loss of constitutional water within the PMo_{12}–SiO_2 hybrid. The latter result indicates the relative difficulty in removal of the water which is contained in PMo_{12} molecules inside the porous silica framework. Therefore, plenty of water is reserved in the porous silica framework which is of importance since the water is essential for efficient electron transfer between phosphomolybdic acid and gas molecules.

X-Ray diffraction measurement

The XRD pattern (Fig. S3, ESI†) of the monolithic pieces are characteristic of a typical diffusion curve (2θ = 3–90°), indicating that the monolithic pieces are amorphous.

Investigation of the gasochromic property

The color change of the monolithic pieces before and after exposure to H_2S gas is clearly shown in Fig. 3. According to Fig. 4, after exposure to H_2S, the hybrid material exhibits the characteristic absorption peaks of phosphomolybdic acid at 228 and 325 nm. The former results from the charge transfer transition from terminal oxygen to molybdenum ($O_d \rightarrow Mo$), and the latter is the charge transfer transition from bridging-oxygen to molybdenum ($O_b/O_c \rightarrow Mo$).[11] However, compared to the UV-Vis spectra of $H_3PMo_{12}O_{40}$ aqueous solution (absorption maxima at 215 and 235 nm), the obvious red shift of absorption maxima for the monolithic pieces is a result of the interaction between the phosphomolybdic acid molecule and the silica network. The chemically active silanol group ($\equiv$Si–OH) is protonated to form the ($\equiv$Si–OH_2^+) group in an acidic medium. The ($\equiv$Si–OH_2^+) group as a counterion of the $PMo_{12}O_{40}^{3-}$ anion could yield a ($\equiv$Si–OH_2^+)$_3$($PMo_{12}O_{40}^{3-}$) pair by acid–base reaction.[12] Furthermore, the broad peak at *ca.* 665 nm is a characteristic absorption of reduced Keggin molecular species with d–d bands.

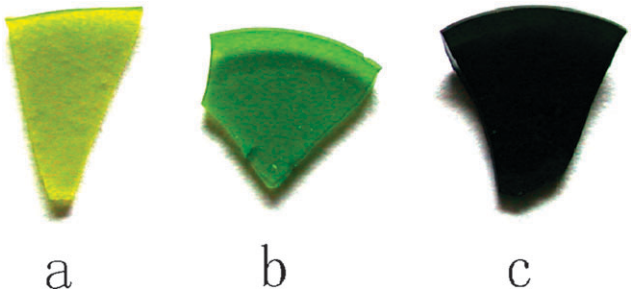

Fig. 3 Digital photographs of the monolithic pieces on contact with 7 mg L^{-1} of H_2S for 0 s (a), 30 s (b) and 300 s (c), respectively. From left to right, the color is yellow, green and dark green.

The gasochromic property of the hybrid material can be well investigated by UV-Vis spectroscopy. Fig. 5(a) depicts gasochromic responses of the PMo_{12}–SiO_2 monolithic pieces with different concentrations of H_2S. The H_2S concentration was varied from 0 to 10 mg L^{-1}, and the sensing time was 1 min. The inset displays the kinetic plots of the gasochromic process of the hybrid material. The H_2S gas was prepared from the reaction $H_2SO_4 + FeS \rightarrow H_2S + FeSO_4$ and dried by $CaCl_2$. Upon exposure to H_2S gas (H_2S is mixed with air of 1 atm), the color of the monolithic pieces changes from transparent yellow to dark green (the green color in the monolithic pieces arises from the coexistence of a blue and a yellow species). Simultaneously, we observe a new broad absorption peak with a maximum at *ca.* 665 nm. The absorption at 665 nm increases gradually with increasing H_2S concentration. The peak is a characteristic absorption of reduced PMo_{12}, owing to the optical absorption of an intervalence charge transfer (IVCT, Mo^{5+} to Mo^{6+}) band at about 769–625 nm.[11] The appearance of the IVCT band indicates that electron transfer occurs

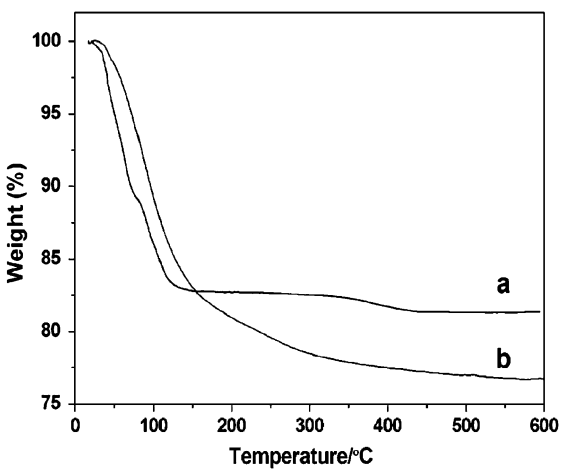

Fig. 2 TGA traces of phosphomolybdic acid (a) and PMo_{12}–SiO_2 hybrid material (b).

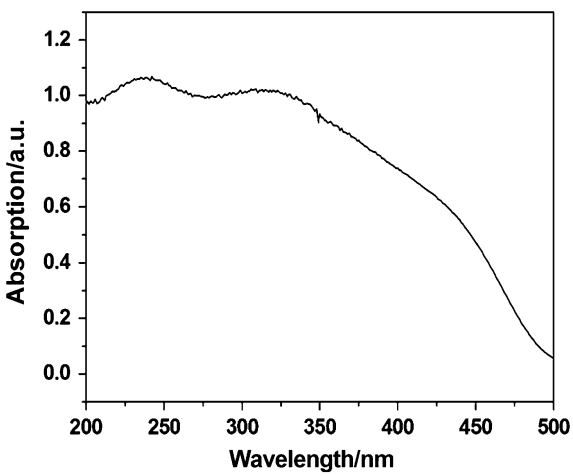

Fig. 4 UV-Vis spectrum of the hybrid material after exposure to H_2S.

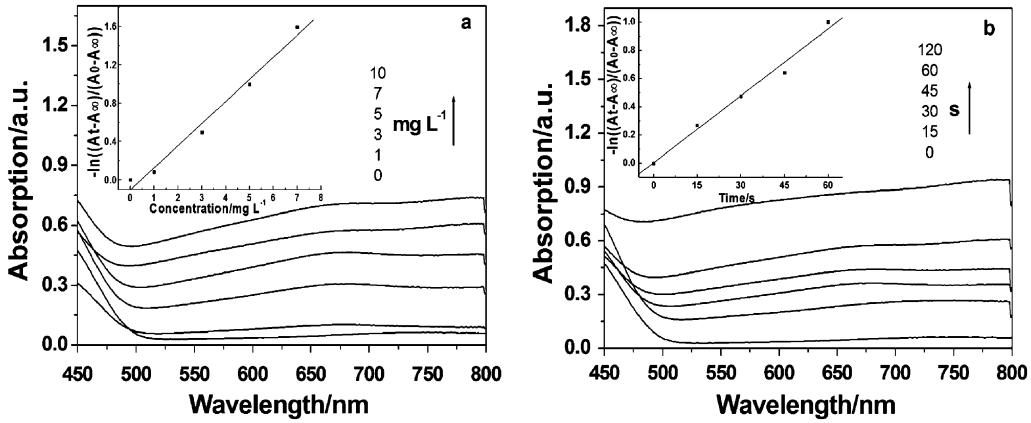

Fig. 5 UV-Vis spectra of the PMo_{12}–SiO_2 hybrid material on exposure to H_2S of different concentrations for 1 min (a) and to H_2S of 7 mg L^{-1} for different exposure times (b). The insets in (a) and (b) show kinetic plots of the gasochromic process of the hybrid material.

between PMo_{12} and H_2S in the silica framework, converting the heteropoly anions to heteropoly blues. Fig. 5(b) shows the gasochromic response of the silica material after exposure to 7 mg L^{-1} of H_2S gas with different exposure times of 0, 15, 30, 45, 60 and 120 s at room temperature. The absorbance at 665 nm increases steadily with prolonged exposure time, confirming the interaction between the porous material and H_2S gas. The gasochromic process fits the first-order kinetic equation based on the linear correlation of $-\ln[(A_t - A_\infty)/(A_0 - A_\infty)]$ *vs.* the exposure time, as shown in the inset of Fig. 5(b). The kinetic constant k is calculated from the slope to be 0.0159 s^{-1}. As determined from the elemental analysis, the relative amount of S which is absorbed by the porous silica material in 120 s is 3.53%.

In order to investigate the reproducibility of the gasochromism, a series of silica materials were prepared under similar conditions. Upon exposure to 7 mg L^{-1} of H_2S in 1 min, all the silica materials turn green, and the average absorption at 665 nm is 0.55, indicating that the sensing material can be fabricated in a reproducible manner. After H_2S gas is removed, the sensing material retains the green color over 30 days in air at room temperature. However, the green silica turns yellow gradually on contact with Cl_2 gas. In order to investigate the reversibility of the coloration–decoloration process, the wavelength of 665 nm was used to observe the changes of absorption for the silica material. First, the absorption of the original silica material was measured. Second, the silica was in contact with 7 mg L^{-1} of H_2S for 1 min and the absorption was also measured immediately. Third, the green silica material was oxidized by Cl_2 and the absorption was measured once again. By repeating the process, Fig. 6 can be obtained showing the reversibility of the coloration–decoloration cycle of the PMo_{12}–SiO_2 hybrid material. However, the absorption of recoloration reaches only *ca.* 0.25 which is lower than that of the original absorption. This cycled coloration–decoloration process can be repeated more than 10 times with little fatigue. It is possible that a small amount of oxidation products are retained in the porous of the silica material, which decreases the gasochromic activity of the material. Therefore the pieces are not reduced deeply by H_2S and can be reoxidized by Cl_2.

We also studied the gasochromic property of the sensing material induced by SO_2. When the silica material was in contact with pure SO_2 gas for 2 min, the gasochromic absorption value reaches to *ca.* 0.38 which is lower than that obtained from H_2S. Obviously, the sensing material requires a higher SO_2 concentration or more exposure time to obtain the same optical absorption as that obtained from H_2S. We believe that the PMo_{12}–SiO_2 hybrid material has higher sensitivity to H_2S than to SO_2, which probably results from the higher reducibility of H_2S.

X-Ray photoelectron spectra

The X-ray photoelectron spectra (XPS) of the PMo_{12}-doped silica were measured to identify the elemental composition and corresponding binding energies. Upon exposure to H_2S, the presence of C, O, Si, P, Mo and S elements in the sample are confirmed by the observed spectral peaks. Furthermore, the expected molar ratio of 1 : 12 for P to Mo can be also approximately established.

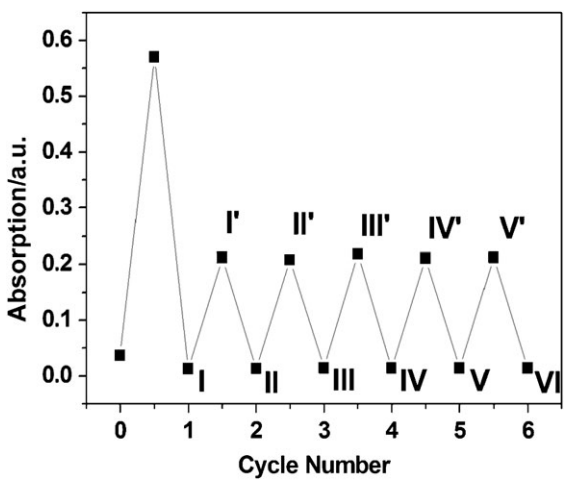

Fig. 6 The absorption changes at 665 nm of the silica material during the coloration–decoloration process. The absorption after exposure to Cl_2 gas (valleys I–VI) returns to the initial value in less than 5 min; the absorption of recoloration (peaks I′–V′) is lower than the initial value.

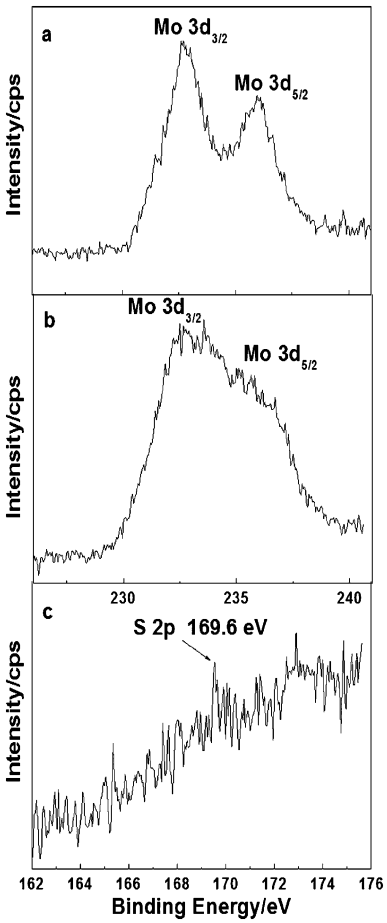

Fig. 7 XPS Measurements in the Mo 3d region of the PMo_{12}–SiO_2 hybrid material (a) before exposure to H_2S and (b) after exposure to H_2S; and (c) in the S 2p region of the silica.

Fig. 7(a) and (b) display the XPS spectra of the Mo 3d level of the PMo_{12}–SiO_2 hybrid material before and after exposure to H_2S. As expected, there are obvious changes for the superposed shape of Mo $3d_{3/2}$ and $3d_{5/2}$ peaks in the XPS spectra before and after exposure to H_2S. It can be seen that, after exposure to H_2S, the Mo $3d_{5/2}$ peak shifts from 235.9 to 235.0 eV, obviously resulting from the presence of Mo(v) component. In addition, Fig. 7(c) displays a S 2p peak with a binding energy of 169.6 eV, indicating that the PMo_{12} oxidizes the H_2S to higher thio-oxy anions, and primarily sulfate (SO_4^{2-}).[9] By the analytical methods mentioned above, it is suggested that PMo_{12} obtains electrons and is reduced to heteropoly blue with simultaneous oxidation of the H_2S to sulfate in the silica framework during the gasochromic process.

FT-IR Spectra

FT-IR Spectroscopy is an effective experimental tool widely used for the characterization and determination of structure and composition of hybrid materials. Fig. 8(a) and (b) present the FT-IR spectra of the acid $H_3PMo_{12}O_{40}$ and silica containing PMo_{12}. The characteristic IR vibration bands of $H_3PMo_{12}O_{40}$ in the region from *ca.* 1000 to 700 cm^{-1}, are assigned to P–O vibration in the central PO_4 unit, and to Mo═O and Mo–O–Mo vibrations, respectively (ESI† Table S1).[11b] As for the silica framework, the characteristic bands mainly appear around 1170 (C–O–C), 1080 (Si–O–Si), 950 (Si–OH) and 800 cm^{-1} (Si–O–Si), indicating the development of a network during the gel formation.[12a] These results demonstrate that PMo_{12} clusters have been incorporated into the porous silica and the basic structure of PMo_{12} is still preserved inside the silica framework, although the bands in the hybrid material are slightly shifted when compared to the bands of phosphomolybdic acid in the KBr pellet. The FT-IR spectrum of the colored silica material (Fig. 8(c)) also showed little change, indicating that the Keggin structure of PMo_{12} is maintained during the gasochromic process. Hence, we consider that the redox reaction during the gasochromic process does not affect the framework of the hybrid material.

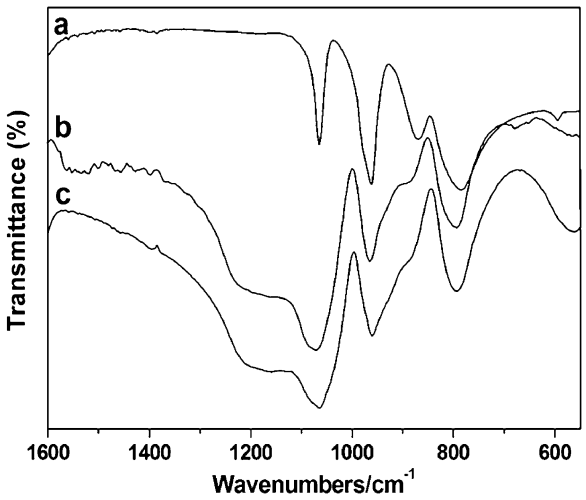

Fig. 8 FT-IR Spectra of the $H_3PMo_{12}O_{40}$ polyanion in a KBr pellet (a), and the PMo_{12}–SiO_2 hybrid material before (b) and after exposure to H_2S (c).

Conclusion

In conclusion, a novel gasochromic hybrid material based on Keggin-type phosphomolybdic acid was fabricated by a sol–gel method. The color of the silica material changed rapidly from transparent yellow to dark green on contact with reducing gases such as H_2S and SO_2. The PMo_{12}–SiO_2 hybrid material can detect H_2S and SO_2 gases without any power consumption at room temperature and was found to exhibit higher sensitivity to H_2S than to SO_2. The gasochromic response is strongly correlated to the reducing ability of the gas. Although both response time and sensibility of the gasochromic material should be improved to achieve the requirements of useful gas sensors, our results open up prospects for developing polyoxometalate-based gasochromic sensing material for practical application.

Experimental

Synthetic procedure of PMo_{12}–SiO_2 hybrid material

The detailed procedure to prepare PMo_{12}–SiO_2 monolithic pieces is as follows: 2.0811 g of tetraethoxysilane (TEOS, 1×10^{-2} mol) were added to 0.5150 g of ethanol (1×10^{-2} mol)

and 0.4800 g distilled water (2.67×10^{-2} mol) under vigorous stirring. The mixture was heated to 60 °C and stirred for about 10 min until a clear solution was obtained. Then 0.3 g of PMo_{12} (1.3×10^{-3} mole) was added to the cooled mixture followed by 1.5 g of deionized water (0.83 mol), and the blend was mixed up to total dissolution of PMo_{12} (about 10 min). After that, yellow transparent monolithic pieces were obtained by placing the mixture in the dark (avoiding light irradiation) at ambient temperature for 15–18 h.

The H_2S and SO_2 gases were prepared in our laboratory. H_2S was prepared in terms of the reaction $H_2SO_4 + FeS \rightarrow H_2S + FeSO_4$ and dried by $CaCl_2$. SO_2 was prepared by the reaction $H_2SO_4 + Na_2SO_3 \rightarrow SO_2 + Na_2SO_4 + H_2O$ and dried by $CaCl_2$. All chemicals were purchased from Sinopharm Chemical Reagent Beijing Co., Ltd. All reagents were analytical grade and used without further purification. The water used in all experiments was deionized to a resistivity of 18 MΩ.

Sensing experiments

Sensing experiments were conducted in a dry 1.3 L flask into which 100–150 mg of PMo_{12}–SiO_2 hybrid material was placed. A certain quantity of pure H_2S (*ca.* 1 atm) was injected into the flask so as to yield a desired concentration, and then the flask was quickly sealed with a stopper. The hybrid material was in contact with the dilute H_2S gas for different times at room temperature. Subsequently, the hybrid material was removed for spectral analysis. The UV-Vis spectra of the silica were thoroughly studied with exposure to different concentrations of H_2S gas for 1 min and to 7 mg L^{-1} of H_2S gas for different time spans.

General

A Cary 500 Scan UV-Vis-NIR spectrophotometer was used to record absorption spectra. FT-IR spectra were measured with a Perkin-Elmer 580B infrared spectrophotometer. X-Ray photoelectron spectra (XPS) were performed on an Escalab MKII photoelectron spectrometer with ALK2 (1486.6 eV) as the excitation source. Thermal gravimetric analysis was performed on a Perkin-Elmer TGA7 instrument in flowing N_2 with a heating rate of 10 °C min^{-1}. The X-ray diffraction (XRD) pattern was collected on a Rigaku D/max-IIB X-ray diffractometer in the range of 3–90° (2θ), employing Cu-Kα radiation (1.542 Å). Elemental analysis of S was done with a VarioEL element analysis instrument.

The electrochemical experiments were performed on a CHI 605C Electrochemical Workstation (Shanghai Chenhua Instrument Corporation, China). A standard three-electrode system was employed with saturated calomel electrode (SCE) as the reference electrode, platinum wire as the counter electrode, and PMo_{12}-modified glassy carbon electrode (GCE) as the working electrode. The surface of the bare GCE was polished with 1.0, 0.3 and 0.05 mm a-Al_2O_3 powder successively and washed with purified water before use. Sonication of the polished electrode appeared to have no effect on the resulting responses. Electrochemistry measurements were conducted in 0.5 M H_2SO_4. A bare glassy carbon electrode was respectively immersed in 1×10^{-3} M of PMo_{12} aqueous solution and PMo_{12}-containing sol, and allowed to stand for 2 h. Then the electrode was taken out and rinsed with deionized water, and the resulting electrode was transferred to 0.5 M H_2SO_4.

Acknowledgements

The authors are thankful for the financial supports from the National Natural Science Foundation of China (Grant No. 20671017; 20731002) and the Specialized Research Fund for the Doctoral Program of Higher Education.

References

1 C. M. Lampert, *Mater. Today*, 2004, **3**, 28–35.
2 L. Zhuang, X. Q. Xu and H. Shen, *Surf. Coat. Technol.*, 2003, **167**, 217–220.
3 (*a*) S. Liu, D. G. Kurth and D. Volkmer, *Chem. Commun.*, 2002, 976–977; (*b*) M. T. Pope and A. Müller, *Angew. Chem.*, 1991, **103**, 56–70; (*c*) E. Coronado, M. Clemente-León, J. R. Galán-Mascarós, C. Giménez-Saiz and E. Martínez-Ferrero, *J. Chem. Soc., Dalton Trans.*, 2000, 3955–3961; (*d*) B. Demirel, S. Fang and E. N. Civens, *Appl. Catal., A*, 2000, **201**, 177–190.
4 (*a*) C. L. Hill, *Chem. Rev.*, 1998, **98**, 1–2; (*b*) M. Sadakane and E. Steckhan, *Chem. Rev.*, 1998, **98**, 219–237; (*c*) M. T. Pope and A. Müller, *Angew. Chem., Int. Ed. Engl.*, 1991, **30**, 34–48.
5 D. Ingersoll, P. J. Kulesza and L. R. Faulkner, *J. Electrochem. Soc.*, 1994, **141**, 140–147.
6 (*a*) G. G. Gao, L. Xu, W. J. Wang, W. J. An and Y. F. Qiu, *J. Mater. Chem.*, 2004, **14**, 2024–2029; (*b*) G. G. Gao, L. Xu, W. J. Wang, W. J. An, Y. F. Qiu, Z. Q. Wang and E. B. Wang, *J. Phys. Chem. B*, 2005, **109**(18), 8948–8953; (*c*) B. B. Xu, L. Xu, G. G. Gao and Y. N. Jin, *Appl. Surf. Sci.*, 2007, **253**(6), 3190–3195.
7 (*a*) S.-D. Choi, W.-Y. Chung and D.-D. Lee, *Sens. Actuators, B*, 1996, **36**, 263–266; (*b*) Y. Shimizu, N. Matsunaga, T. Hyodo and M. Egashira, *Sens. Actuators, B*, 2001, **77**, 35–40; (*c*) R. Ionescu, A. Hoel, C. G. Granqvist, E. Llobet and P. Heszler, *Sens. Actuators, B*, 2005, **104**, 124–131; (*d*) Y. L. Liu, H. Wang, Y. Yang, Z. M. Liu, H. F. Yang, G. L. Shen and R. Q. Yu, *Sens. Actuators, B*, 2004, **102**, 148–154.
8 M. Xu, Y. C. Li, W. L. C. Q. Sun and L. X. Wu, *J. Colloid Interface Sci.*, 2007, **315**, 753–760.
9 (*a*) M. K. Harrup and C. L. Hill, *Inorg. Chem.*, 1994, **33**, 5448–5455; (*b*) M. K. Harrup and C. L. Hill, *J. Mol. Catal. A: Chem.*, 1996, **106**, 57–66.
10 V. Wittwer, M. Datz, J. Ell, A. Georg, W. Graf and G. Walze, *Sol. Energy Mater. Sol. Cells*, 2004, **84**, 305–314.
11 (*a*) G. J. Zhang, Z. H. Chen, T. He, H. H. Ke, Y. Ma, K. Shao, W. S. Yang and J. N. Yao, *J. Phys. Chem. B*, 2004, **108**, 6944–6948; (*b*) T. R. Zhang, W. Feng, Y. Q. Fu, R. Lu, B. Zhao and J. N. Yao, *J. Mater. Chem.*, 2002, **12**, 1453–1458.
12 (*a*) Y. H. Guo, Y. H. Wang, C. W. Hu and E. B. Wang, *Chem. Mater.*, 2000, **12**, 3501–3508; (*b*) I. V. Kozhevnikov, K. R. Kloetstra, A. Sinnema, H. W. Zandbergen and H. Van. Bekkum, *J. Mol. Catal.*, 1990, **114**, 287–298; (*c*) V. M. Mastikhin, S. M. Kulikov, A. V. Nosov, I. V. Kozhevnikov, I. L. Mudrakovsky and M. N. Timofeova, *J. Mol. Catal.*, 1990, **60**, 65–70.